

RSC Advances



This is an *Accepted Manuscript*, which has been through the Royal Society of Chemistry peer review process and has been accepted for publication.

Accepted Manuscripts are published online shortly after acceptance, before technical editing, formatting and proof reading. Using this free service, authors can make their results available to the community, in citable form, before we publish the edited article. This *Accepted Manuscript* will be replaced by the edited, formatted and paginated article as soon as this is available.

You can find more information about *Accepted Manuscripts* in the [Information for Authors](#).

Please note that technical editing may introduce minor changes to the text and/or graphics, which may alter content. The journal's standard [Terms & Conditions](#) and the [Ethical guidelines](#) still apply. In no event shall the Royal Society of Chemistry be held responsible for any errors or omissions in this *Accepted Manuscript* or any consequences arising from the use of any information it contains.

Photo-inhibition of A β fibrillation mediated by a newly designed fluorinated oxadiazole.

M.R. Mangione^{a,*}, A. Palumbo Piccionello^{a,b,c*}, C. Marino^{a,d}, M.G. Ortore^e, P. Picone^f, S. Vilasi^a, M. Di Carlo^f, S. Buscemi^{a,b}, D. Bulone^a and P.L. San Biagio^a.

a Institute of Biophysics, National Research Council, Palermo, Italy, **b** Department of biological chemical and pharmaceutical sciences and technologies, University of Palermo, Palermo, Italy, **c** Euro-Mediterranean Institute of Science and Technology, Palermo, Italy, **d** Department of Neurology, University of Texas Medical Branch, Galveston, (TX) USA, **e** Department of Life and Environmental Sciences and National Interuniversity Consortium for the Physical Sciences of Matter, Marche Polytechnic University, Ancona, Italy, **f** Institute of Biomedicine and Molecular Immunology, National Research Council, Palermo, Italy.

* The two authors have contributed equally to the present work

[†] Corresponding author

ABSTRACT: Uncontrolled aggregation of amyloid beta peptide (A β) is the main cause of Alzheimer's Disease. Therapeutic approaches of intervention in amyloid diseases include the use of small molecules able to stabilize the soluble A β conformation, or to redirect the amyloidogenic pathway towards non-toxic and non-fibrillar states. Fluorometric measurements revealed that the 3-(4'-trifluoromethylphenyl)-5-(4'-methoxyphenyl)-1,2,4-oxadiazole, when irradiated, is able to interact with the monomeric A β peptide readdressing the aggregation pathway toward the formation of amorphous aggregates as evidenced by CD, AFM, and SAXS measurements. We hypothesize that this compound, under radiation, forms a reactive intermediate that sticks on the A β peptide by interfering with its fibrillation process. Cytotoxicity assays performed on LAN5 neuroblastoma cells suggest that the presence of oxadiazole reduces the toxicity of A β . This finding might be the starting of innovative therapies against Alzheimer's Disease.

KEYWORDS: Alzheimer's disease, Amyloid, Fibrillation inhibition, Photo-excitation, Neuronal diseases.

Introduction

Alzheimer's Disease (AD) is a neurodegenerative pathology representing the most common form of dementia in the elderly. The affected individuals present progressive loss of memory, mood changes, communication and reasoning problems¹⁻³. The pathology is characterized by the formation of extracellular amyloid plaques and intracellular neurofibrillary tangles in the brain⁴. All these deposits are composed by well-ordered, β -sheet rich, fibers of the Amyloid β peptides (A β) produced by proteolysis of Amyloid Precursor Protein (APP) in residues of 39-43 amino acids. The evidence of the simultaneous presence of accumulated fibers and the cerebral tissue loss brought to the initial hypothesis that the proteinaceous aggregates are responsible for the neurodegenerative damage⁵⁻⁷. However, it has been shown that the species formed in the initial state of the aggregation kinetic could determine severe damage in the cerebral cells⁸⁻¹⁰. Many experimental evidence, in fact, highlighted the role of these species in the alteration of membranes, particularly of their solubility and permeability^{11, 12}. Moreover, the pathological presynaptic alteration was observed in transgenic mice brain before the neuronal degeneration associated to fibers accumulation. These

observations suggest that the severity of the pathology is uncorrelated with the concentration of the mature fibers¹³⁻¹⁷. Despite many efforts and numerous studies conducted, the mechanism and the pathogenesis of AD are still matter of debate. The problem is also compounded by the instability of the peptide both in the monomeric and early aggregated form and by the presence of numerous polymorphic aggregates and fibers. In fact, A β aggregation is a complex process that seems to involve more than a simple conversion from an unstable monomer to mature fibrils^{18, 19}.

Some therapeutic approaches trigger the disaggregation of the amyloid deposits and aggregates. Graphene-based materials or gold nanoparticles, with high affinity for deposits of A β fibers, were used to redissolve them, by using the local heat²⁰⁻²².

Over the last years, increasing interest has been focused on the study of natural or synthetic molecules capable of interfering with the aggregation and fibrillation of A β peptide²³⁻²⁵. The search of small inhibitors of the toxic effects of A β has produced a wide number of approaches and promising drugs²⁶⁻³².

Particularly, growing interest has been addressed to molecules able to drive the unstable monomers towards the formation of

harmless and stable aggregates³³. Indeed, the deviation of the aggregation mechanism toward off-pathway products seems to be a new promising strategy for the treatment of amyloid diseases.

For example, the inhibitor effects of curcumin on the fibrillation have been investigated by different authors^{25, 27, 34, 35}. Curcumin is a natural molecule characterized by anti-inflammatory and antioxidant activity. However, it crosses the blood-brain barrier (BBB) only when injected, and its effectiveness is reduced when added to the diet^{36, 37}. These limitations have prompted the synthesis of new derivatives having a major efficacy on the inhibition of aggregation^{38, 39}.

The Ferulic acid is another example of natural molecule with *in vitro* inhibitory activity. In fact, this molecule seems to interfere with the oligomer formation through the destabilization of Asp23-Lys28 salt bridge that is at “the basis of fibril stability”^{40, 41}.

All these compounds share a common phenolic structure that seems to be responsible for the fibril destabilization.

A new branch of research in this field aims to the control of the amyloid aggregation through photochemical methods. For instance, it has been synthesized a “photo-clickable” A β ₁₋₄₂ peptide with increased stability and solubility, whose primary structure is earned after photo-stimulation³⁹. Very recently, the photochemical approach also allowed to control the peptide aggregation by means of riboflavin-mediated photooxygenation of A β ₁₋₄₂, resulting into a decrease of Abeta toxicity and a reduction of the uncontrolled self-assembly^{42, 43}.

The photo-stimulation is also used to trap, detect and characterize low molecular weight oligomers of A β -peptide using the PICUP technique (photo-induced protein cross-linking of unmodified proteins). This intriguing photo-chemical method seems to be well appropriate for structural studies of the transient and dynamic equilibrium between small oligomeric species of A β ⁴⁴. A characteristic of this technique is the short irradiation time required (few seconds) because of the involved metal complexes characterized by high photo-reactivity. However the short time of irradiation can make somehow difficult to redirect accurately the aggregation pattern toward the formation of small oligomers⁴⁴. Moreover, the toxicity of involved metal complexes avoids the perspective of pharmaceutical development.

In this context, we decided to design a new not toxic photo-active molecule able to interact with A β in order to modulate its aggregation pattern by means of photo-stimulation.

Recent studies indicated 1,2,4-oxadiazoles as promising probes for detection of amyloid plaques *in vivo* due to their high affinity toward A β ⁴⁵. These interesting heterocycles, utilized in many pharmaceutical applications⁴⁶⁻⁴⁹, present a well known photochemical reactivity^{50, 51} characterized by the formation of intermediates able to induce by photostimulation an electron transfer (PET) with amines or an energy transfer (ET) with aromatic species⁵²⁻⁵⁴. In this study we designed, synthesized, characterized and tested a new fluorinated oxadiazolic compound which interfere with the A β self-assembly. The activation of the oxadiazolic compound at an appropriate

wavelength is responsible for the formation of photo-active species exerting an inhibitory effect on A β fibrillation. Our experimental investigations were achieved by means of different techniques that are fluorescence, circular dichroism (CD), atomic force microscopy (AFM), and small angle x-ray scattering (SAXS). We aim to evidence with different structural resolutions the effects of the compound on A β aggregation pathway. Finally, preliminary investigation relative to the toxicity of the oxadiazolic compound were also examined by *in vitro* cellular experiments.

Materials and methods

Synthesis of 3-(4'-trifluoromethylphenyl)-5-(4'-methoxyphenyl)-1,2,4-oxadiazole.

Pyridine (1.1 eq.) and 4-methoxybenzoyl chloride **2** (1.1 eq.) were added to a suspension of 4-trifluoromethylphenylamidoxime **1** (4.9 mmol, 1.0 g) in toluene (100 mL). The reaction mixture was refluxed for 8 hours. The solvent was removed under reduced pressure and the residue was chromatographed giving compound **3** (84%).

3-(4'-trifluoromethylphenyl)-5-(4'-methoxyphenyl)-1,2,4-oxadiazole 3: mp 145-147°C. FT-IR (nujol) ν : 1613 cm⁻¹. ¹H NMR (300 MHz, CDCl₃) δ : 3.92 (s, 3H, OCH₃), 7.78 (d, J = 6.9 Hz, 2H, Ar), 7.83 (d, J = 8.1 Hz, 2H, Ar), 8.17 (d, 2H, J = 6.9 Hz, Ar), 8.26 (d, 2H, J = 8.1 Hz, Ar). GC-MS (m/z): 320 (M+, 100%). Elemental analysis for C₁₆H₁₁F₃N₂O₂ Teor: C, 60.00; H, 3.46; N, 8.75. Exper: C, 60.03; H, 3.48; N, 8.78.

Sample preparation. The oxadiazole was solubilized in ethanol at 1 mM concentration and then diluted to 10 μ M in 10 mM phosphate buffer (PB) solution (NaH₂PO₄/Na₂HPO₄-RIEDEL DE HAEN- in water -MilliQ-) at pH 7.4.

The lyophilized synthetic peptide A β ₁₋₄₀ (Polypeptide) was solubilized with NaOH 5 mM (Sigma-Aldrich), pH 10, sonicated and already lyophilized according to Fezoui et al. treatment⁵⁵. After this procedure the peptide was dissolved in PB 10 mM and then filtered with two filters in series having diameter of 0.20 μ m (Whatman) and 0.02 μ m (Millex-Lg) respectively, in order to eliminate whatever aggregates. The sample preparation was operated in a cool room at 4°C. A β concentration (50 μ M for all samples) was determined by tyrosine absorption at 276 nm using an extinction coefficient of 1390 cm⁻¹M⁻¹.

The aggregation kinetics were followed at controlled temperature (37°C) and under stirring (200 rpm) for 24 hours. Samples prepared for AFM images were aged at 37°C for 4 days before the deposition on the mica surface. The same aged samples were concentrated at 150 μ M using Millipore filters with a cut-off of 3 kDa before X-ray scattering measurements, in order to obtain the necessary scattering intensity. Samples for cytotoxicity assays were collected at 0, 5 and 24 hours of kinetic experiments in order to select aggregates at different states. All withdrawals were performed using a laminar flow hood to keep sterility.

Spectrofluorometric measurements. Emission spectra were recorded using a spectrofluorometer Jasco FP-6500. The oxadiazole emission spectra was recorded in ethanol and in PB/EtOH 99:1 using a quartz cell with 10 mm path length. The wavelength of excitation was 260 nm and the emission range was 250-500 nm.

Circular Dichroism spectroscopy. The secondary structure of the A β ₁₋₄₀ was studied by using a JASCO J-815 CD Spectrometer. Particularly, withdrawals of samples at appropriate time during the aggregation kinetic were observed. Spectra were recorded at 20°C using a quartz cell with 0.2 mm path length. Each spectrum measurement was obtained by averaging over eight scans and subtracting the blank solvent contribution.

AFM analysis. Aliquots of 50 μ M representative samples at the end of the aggregation kinetics were deposited onto freshly cleaved mica surfaces (Agar Scientific, Assing, Italy) and incubated for up to 2 minutes before rinsing with deionized water and drying with gentle nitrogen flow. AFM experiments were achieved with a Nanowizard II system (JPKInstruments, Germany), operating in tapping mode in air and at room temperature. Single beam silicon cantilevers (TESPA, NanoAndMore, USA) with a nominal spring constant of 42 N/m and resonance frequency of 320 kHz, were used. Images with scan sizes of 2x2 μ m² were acquired on different areas on each sample. Analysis of the aggregates size was performed by using the data processing software provided by JPK Instruments.

Small Angle X-ray Scattering. SAXS experiments were performed at ID2 beamline at the European Synchrotron Radiation Facility in Grenoble, France. The sample temperature was maintained at 20 °C. SAXS patterns were recorded using a fiber optically coupled two-dimension detector, FReLoN (Fast-Readout, Low-Noise). The distance from the sample and the detector was set to 1.5 m, in order to obtain a Q-range ($Q = 4\pi \sin \theta/\lambda$, where 2θ is the scattering angle and $\lambda = 0.995 \text{ \AA}$ the X-ray wavelength) from 0.01 to 0.34 \AA^{-1} . We recorded simultaneously the incident and transmitted intensities to the purpose of obtaining data in an absolute scale, hence the normalized SAXS patterns were azimuthally averaged to obtain the one-dimension profiles of scattered intensity. The buffer contribution was subtracted from protein solution data for each investigated condition, considering the correction for the protein volume fraction. To prevent radiation damage, all solutions were degassed before transferring into the capillary. Each measurement was performed for 100ms, and followed by a dead time of 3s in order to avoid radiation damage. This strategy was repeated for 50 times in order to obtain a satisfactory signal-to-noise ratio, despite the low protein concentration which was investigated.

Cell cultures, treatment and cell viability determination.

Cells were cultured in 96 well plates at 1,5 x10⁶ cells per well in RPMI 1640 medium (Celbio srl, Milan, Italy) supplemented with 10% fetal bovine serum (Gibco-Invitrogen, Milan, Italy) and 1% penicillin, 1% streptomycin (50 mg ml). Cells were maintained in a humidified 5% CO₂ atmosphere at 37°C. LAN5 cells were treated for 72h with samples of A β without or with compound **3** taken according to sample preparation. The final concentrations were 6.25 μ M for A β and 1.25 μ M for **3**. Cell viability was measured by MTS assay (Promega Italia, S.r.l., Milan, Italy). MTS [3-(4,5-dimethylthiazol-2-yl)-5-(3-carboxymethoxyphenyl)-2-(4-sulphophenyl)-2H-tetrazolium] was utilized according to the manufacturer's instructions. After cell treatments, 20 μ L of the MTS solution was added to each well, and the incubation was continued at 37°C for 4 hrs. The absorbance was read at 490 nm on the Microplate reader WallacVictor 2 1420 Multilabel Counter (PerkinElmer, Inc. Monza, Italy). Results were expressed as the percentage MTS reduction in the control cells. The control and treated cells were morphologically analyzed by microscopy inspection using Axio scope 2 microscope (Zeiss).

Results and discussion

Synthesis and photochemical characterization of 1,2,4-oxadiazole **3**.

The compound 3-(4'-trifluoromethylphenyl)-5-(4'-methoxyphenyl)-1,2,4-oxadiazole **3** was synthesized accordingly to the general scheme of the amidoxime route, by refluxing the trifluoromethylbenzamidoxime **1** with the appropriate benzoyl chloride in the presence of pyridine (Figure 1).

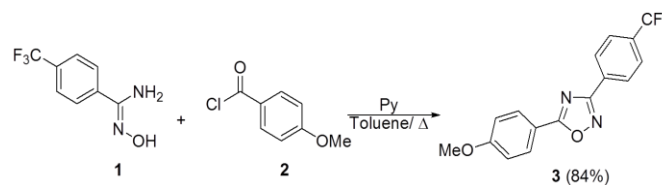


Figure 1: Synthesis of 1,2,4-oxadiazole **3**.

The photochemical features and photostability of this compound were studied by time course measurement of fluorescence emission spectra in different solvents. The Figure 2A shows the kinetic evolution of the emission spectrum of 1,2,4-oxadiazole **3** diluted in ethanol. The emission spectra present a Gaussian-like shape characterized by a time-dependent emission quenching.

Otherwise the oxadiazole dissolved in a solution of PB/ethanol at 99:1 ratio, has an emission spectra (Figure 2B) with an initial intensity quench coupled with a change of the shape. In detail, the emission signal, after about 45 minutes, shows a fine

structure with 3 characteristic bands: an hypsochromic band around 340-350 nm, an halfway band around 360 nm and a bathochromic band near 380 nm.

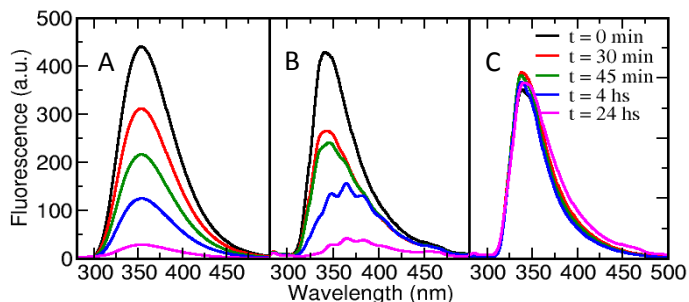


Figure 2: Emission spectra at different kinetic times of compound **3** (10 mM) in: (A) ethanol with continue photo-excitation; (B) in PB:Ethanol (99:1) with continue photo-excitation; (C) in PB:Ethanol (99:1) without continue photo-excitation.

To investigate if the well-known photochemical reactivity of oxadiazoles⁵⁰⁻⁵⁴ is due to the photo-excitation, a sample was incubated at 37°C under stirring (200 rpm) in dark conditions. Interestingly, the emission spectra of sample registered at different times starting from the dissolution in phosphate buffer (Figure 2C) display minor changes in intensity and shape. Overall, these results indicate that while the solvent is responsible for the emission maximum shift, the appearance of a fine structure in aqueous solution is a secondary phenomenon due to photostimulation of the compound.

A similar photochemical behavior has been already observed in cyanine dyes^{56, 57}, and correlated with the strong inter- and intra-molecular interactions of these molecules in aqueous solvent. In fact, it has been suggested that the kinetic evolution of the cyanine emission spectra is correlated to the formation of aggregates. Unlike cyanine dyes, spectral change of oxadiazole are instead induced by photo-excitation. We hypothesize that the oxadiazole ring may easily form a photoactive derivative under the high electronic stress induced by photo-stimulation. Furthermore, the three bands observed in the spectrum, could be related to the formation of aggregates composed by the same photo-excited derivatives but with different slippage angle⁵⁷.

Interaction between 1,2,4-oxadiazole **3** and Amyloid peptide.

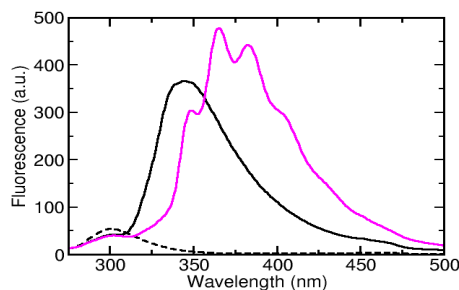


Figure 3: A β_{1-40} (dotted line), A β_{1-40} with the oxadiazole **3** at the initial step (black line) and at the end (pink line) of kinetic with continuous photostimulation.

Reaction conditions: T= 37°C, stirring at 200 rpm, λ_{exc} = 260 nm.

The interaction between 1,2,4-oxadiazole **3** and A β_{1-40} was investigated both with and without photo-stimulation with different experimental techniques. The formation of amyloid fibers was induced by following a method previously described⁵⁸ that assures reproducible results. Briefly, a solution of A β_{1-40} monomers at 50 μ M concentration in 10 mM PB was incubated at 37°C under stirring at 200 rpm. In these conditions the fibrillation started up in about 5 hours, as suggested by ThT assay and CD spectra (see supplementary information). The same incubation protocol was applied to a sample of monomeric A β_{1-40} in presence of the oxadiazolic compound. The fluorescence emission spectrum evolution under continuous irradiation at 260 nm has been followed. Figure 3 shows the spectra recorded at the start and at the end of the kinetic study. The fine structure developed over time is quite similar to that observed in the sample of 1,2,4-oxadiazole **3** alone (Figure 2B). A higher intensity of emission was reached in 12 hours and after that the signal remained stable for a long time (1 month). We suggest that the increase of the signal might be related both to an increased solubility of the aromatic compound in presence of the peptide and to a direct interaction with A β . The latter phenomenon could be accounted for the high affinity of the 1,2,4-oxadiazole for the amyloid protein already observed in the case of similar compounds⁴⁵. On the opposite, the initial and final spectra recorded for the same sample incubated without photo-excitation present minor spectral changes without any appearance of fine structure (Figure 4), thus confirming implication of a photo-reaction.

To verify the oxadiazole effect on the aggregation pathway of A β_{1-40} , the peptide's secondary structure was inspected by CD measurements. Figure 5 shows the dichroic spectra, for both irradiated and not irradiated samples, at the start and at the end of the aggregation kinetics.

Furthermore, CD spectra for a sample of A β alone at the starting and final time steps are also presented for comparison. No change in the typical signal of random coil structure of the monomeric peptide was observed for the sample kept under continuous photo-excitation (red line) while a signal of β -sheet structure formation was found for all other cases. Therefore, the 1,2,4-oxadiazole **3** seems to inhibit the formation of amyloid fibers only when activated by photo-excitation.

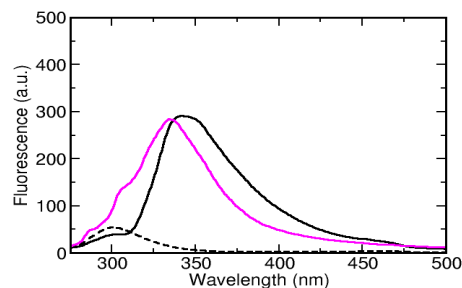


Figure 4: A β_{1-40} (dotted line), A β_{1-40} with the oxadiazole **3** at the initial step (black line) and at the end (pink line) of kinetic without continuous photostimulation.

Reaction conditions: T= 37°C, stirring at 200 rpm, λ_{exc} = 260 nm.

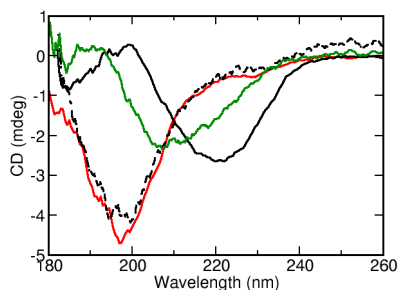


Figure 5: CD spectra for Aβ₁₋₄₀ at initial time (dotted line); final spectra of: Aβ₁₋₄₀ (black curve), Aβ₁₋₄₀ with **3**, without excitation (green curve), Aβ₁₋₄₀ with **3**, under irradiation, λ_{exc} = 260 nm (red curve).

AFM and SAXS measurements performed on samples irradiated and opportunely treated (see sample information for details) confirm the previous results. As shown in Figure 6, amyloid fibers are visible in a sample of Aβ₁₋₄₀ alone incubated at 37°C (Figure 6A), whereas only small aggregates, with a disordered secondary structure, are present when Aβ₁₋₄₀ was incubated at 37°C in presence of compound **3** under continuous photo-excitation (Figure 6B). Structural differences between the two samples are also evidenced by SAXS measurements, as shown in Figure 7.

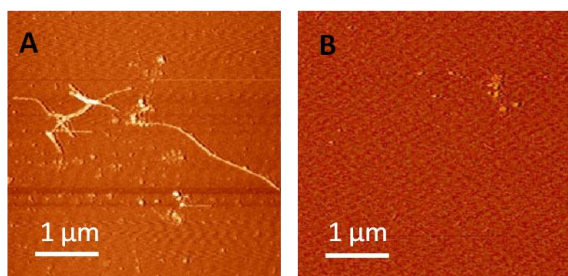


Figure 6: AFM images at the final stage for Aβ₁₋₄₀ (A) and for Aβ₁₋₄₀ with **3** prepared under photo-stimulation (B).

First of all, the macroscopical differential cross section at $Q \approx 0$, which is proportional to the molecular weight of the macromolecules in solution⁵⁹, clearly indicates that the photoexcited sample presents aggregates at lower aggregation numbers. The whole shape of SAXS curves of the two samples is significantly different, as it can be appreciated by their representation in the form of Kratky plot⁶³ (see Figure S2 in the supporting information), too. In fact, while Kratky plot corresponding to Aβ sample alone presents the bell shape indicating the presence of compact objects in solution, the same plot related to Aβ sample with **3** under irradiation is typical of flexible, hence disordered molecules. Hence, Kratky plots determine that Aβ structural features in solution are in agreement with the information provided by AFM images (Fig. 6). In view of these findings, SAXS data corresponding to Aβ sample alone were also represented in the form of modified

Guinier plot for elongated objects⁶³, suggesting the presence of cylinders whose average cross section is about 37 Å (see Figure S3 and related caption in the supporting information). In light of what we have shown up to this point, SAXS curve of Aβ sample alone was successfully fitted considering the presence of mature fibrils that can be approximated to cylindrical objects. The theoretical fitting, reported as a continuous line in the left panel of Figure 7, corresponds to cylinders of length $l = (900 \pm 50) \text{Å}$ and average radius $r_a = (38 \pm 4) \text{Å}$, which results to be poly-dispersed. We stress that the fitting procedure also takes into account Aβ₁₋₄₀ nominal concentration, because scattering data were obtained in absolute scale, according to the same approach reported in literature⁶⁰. The average radius is in agreement with literature results which claim that Aβ₁₋₄₀ fibrils have constant apparent diameters of $(70 \pm 1) \text{Å}$ ⁶¹, and the resulting polydispersity is confirmed by AFM image shown in Figure 6A.

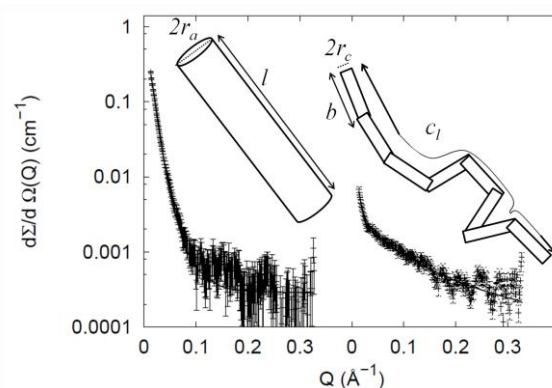


Figure 7: SAXS experimental data and theoretical fitting (continuous lines) obtained at the final stage for Aβ₁₋₄₀ (right) and for Aβ₁₋₄₀ with **3** prepared under photostimulation (left).

On the other side, SAXS curve corresponding to the photo-excited sample cannot be fitted considering cylindrical or other compact objects in solution, as it was inferred by its representation in the form of Kratky plot (Figure S2)⁶². The macroscopical differential scattering cross section was hence adequately fitted by considering the presence of flexible molecules, as illustrated in the sketch of Fig. 7. Particularly, the theoretical curve reported in the right panel of Figure 7 was obtained by considering the Pedersen-Schurtenberger worm-like chain form factor, $P_{PS}(Q)$, multiplied by a two-electron density level cross section for the protein chain^{60, 63},

$$\frac{d\Sigma}{d\Omega}_{\text{wik}}(Q) = \frac{cN_A}{M_{A\beta}} r_e^2 4\pi^2 c_l^2 \left\{ (\rho_{A\beta} - \rho_s) r_c^2 \frac{J_1(Qr_c)}{Qr_c} + (\rho_s - \rho_0)(r_c + \delta) \frac{J_1[Q(r_c + \delta)]}{Q(r_c + \delta)} \right\}^2 P_{PS}(Q) \quad (\text{Eq.1})$$

where N_A is Avogadro's number and r_e is the electron scattering length. According to this model, the cross-sectional radius of the chain r_c , the contour length of the chain c_l , the statistical segment (Kuhn) length representing the separation between two adjacent rigid scattering domains b , considered in the

expression for $P_{PS}(Q)$, and the thickness δ and electron density ρ_s of the surrounding shell, are the fitting parameters. Solvent electron density ρ_0 , $A\beta_{1-40}$ concentration c , its molecular weight $M_{A\beta}$ and electron density $\rho_{A\beta}$ are fixed according to experimental conditions (c) and literature values. The aggregation number N_{agg} represents the number of $A\beta$ monomers that form the flexible chain and can be simply determined by the ratio $\pi r_c^2 c / V_{A\beta}$, where $V_{A\beta}$ is $A\beta_{1-40}$ monomer volume. The theoretical fitting on the experimental SAXS curve reported in the right panel of Figure 7 was performed by considering the simultaneous presence of two species of worm-like chains, as it could be suggested by observing the change of slope of the SAXS curve in the region of $Q \approx 0.03 \text{ \AA}^{-1}$, according to:

$$\frac{d\Sigma}{d\Omega} = x_1 \left. \frac{d\Sigma}{d\Omega} \right|_{w1k1}(Q) + x_2 \left. \frac{d\Sigma}{d\Omega} \right|_{w2k2}(Q) \quad (\text{Eq. 2})$$

where x_1 and x_2 account for the fractions of protein molecules occurring as worm-like species 1 and 2, respectively. However, in order to limit the number of the fitting parameters, only the aggregation number N_{agg} , was left as a free parameter, while the structural parameters r_c and b were considered to be common to both the worm-like species. All the theoretical fitting of SAXS curves were performed by GENFIT software package⁶⁴. The resulting parameters are reported in Table 1, including the weight fraction of each worm-like population.

TABLE 1. Fitting parameters of the SAXS curve corresponding to the photoexcited sample, reported in Figure 7, right panel.

	Aggregation number N_{agg}	Chain radius r_c (Å)	Kuhn length b (Å)	Weight fraction x (%)
Worm-like 1	2.0±0.4	4.3±0.3	10±2	30±5
Worm-like 2	11.2±0.5			70±5

The aggregation numbers and the low value of the cross section radius confirm that the photo-excited sample does not present big aggregates, as evidenced by AFM images. Moreover, the shortness of the statistical segment length is consistent with the lack of secondary structure revealed by CD results.

The mechanism of inhibition of the oxadiazolic compound on $A\beta$ fibrillogenesis could be traced to its photo-reactivity. We hypothesize that the photo-stimulation induces the formation of a reactive intermediate. The latter may react with the $A\beta_{1-40}$ amino acid backbone through an electron and/or energy transfer mechanism and induce a structural modification responsible for fibrillogenesis inhibition, as pictorially represented in Figure 8.

We suggest a mechanism analogous to the PICUP method used for stabilizing metastable amyloid oligomers previously

described⁴⁴. More in details, the method is based on the photo-stimulation of ruthenium or palladium complexes which form radicals capable of extracting an electron from nearby amyloid peptides. The formed reactive species of $A\beta$ may carry out an alternative cross-linking with other neighboring $A\beta$ peptides⁴⁴. Particularly, we suggest that the electron-transfer from Tyr residues could initially generate the coupling of two peptide chain, forming a cross-linked dimers.

We would like to stress that a PICUP-like mechanism is strongly suggested by finding that the oxadiazolic compound exerts an inhibitory effect only under photo-stimulation. Obviously, further experiments will clarify the specific molecular mechanism behind the interaction between amyloid peptide and the oxadiazolic compound.

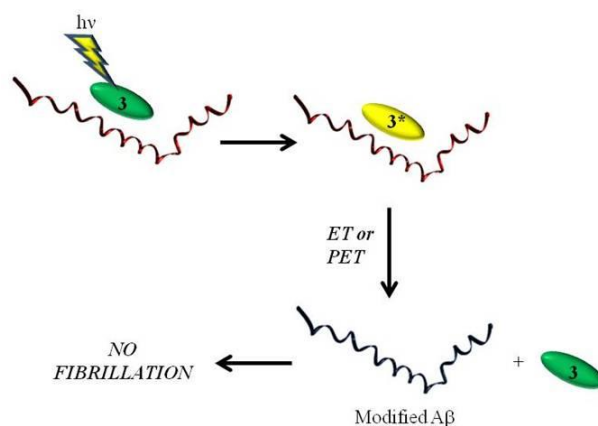


Figure 8: Pictorial representation of photoinduced $A\beta_{1-40}$ modification.

In vitro Cytotoxicity assay

We further investigate the cytotoxicity of compound **3** and its possible effect on the formation of neurotoxic $A\beta_{1-40}$ aggregates, MTS assay was realized on LAN5 neuroblastoma cell line.

LAN5 cells were treated using sample withdrawals taken at 0, 5 and 24 hours of aggregation kinetic of $A\beta_{1-40}$ alone or in presence of the oxadiazole **3**, and their viability was estimated. As shown in Figure 9A, the main toxicity was caused by the sample of $A\beta_{1-40}$ alone incubated for 5 hours, which, accordingly to our previous studies⁵⁸ should contain only oligomeric species. The $A\beta_{1-40}$ sample at the initial time and the fibers obtained after 24 hours do not result as toxic as the **3** compound. To verify the effect of oxadiazole **3** on the toxicity of $A\beta_{1-40}$ photo-stimulated samples for 5 and 24 hours in presence of the compound **3** were dosed on LAN5 cells. No toxic effect was observed for cells treated with samples incubated 5 hours. On the contrary, the samples photo-stimulated for 24 hours cause a reduction on the cell viability if compared with $A\beta$ fibers. However the species formed after this

irradiation time result less toxic if compared with A β aggregates obtained after 5 hours. This evidence suggests a different structural organization obtained in presence of photo-stimulated compound **3**. Microscopic images acquired on the same samples, before MTS assay, showed different cell morphology (Figure 9B), consistently with cell viability results. In fact, LAN5 cells treated with A β_{1-40} alone incubated for 5 hours, presented a reduction of the cellular body and a decrease of a neuritis and neuronal cell number with respect to the control (Figure 9B). On the opposite a regular neuronal morphology is evident for the other samples, included the cells treated with A β -**3** incubated for 24 hours..

On the whole, these results support the hypothesis that the oxadiazole **3** is able to modulate the aggregation pathway of A β peptide and to inhibit the formation of toxic oligomer if properly photo-stimulated .

irradiation time. Although this photo-stimulated compound cannot be used, at this stage, as the direct drug for AD treatment, we consider our results a crucial step to elucidate the molecular specific mechanism of action of small stabilizing molecules. Furthermore, we suggest that the compound **3** could be used to build new technological and experimental strategies in this direction. In fact, very interesting is the possibility, offered by our study, to use the compound **3** for the production of non-toxic oligomers. In fact, it is known, that the study of amyloid oligomers structure requires their easy production. In this respect, the production of stable oligomers induced by the A β_{1-40} peptide interaction with the photo-stimulated compound **3**, has been tested and it could be an attractive possibility to finely tuning in a photo-catalytic way this production. The atoxic profile of compound **3** suggests the further development of 1,2,4-oxadiazole derivatives that could be photo-stimulated with NIR light for the practical perspective development of a photo-therapy for AD.

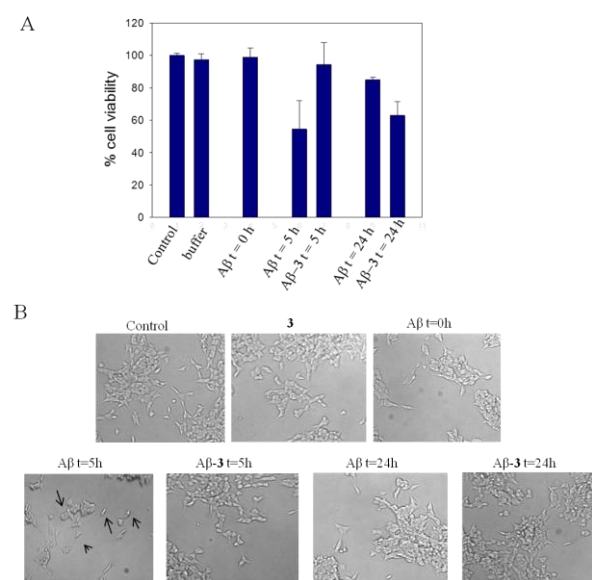


Figure 9: A) Viability for LAN5 cells after 72 h of incubation with sample at different kinetic time of A β_{1-40} (t = 0, 5, and 24 h) and A β_{1-40} with oxadiazole **3** (t = 5, and 24h) compared with control and oxadiazole **3**. B) Microscopic images for cells treated with same.

Conclusion

Uncontrolled aggregation of amyloid beta peptide is the main cause of Alzheimer's Disease^{1, 2}. In the last years the attention has been focused on the potential use of small molecules for stabilizing or redirecting the amyloidogenic pathway towards the non-toxic and non-fibrillar states. In this work, we present the newly designed compound **3**, namely (3-(4'-trifluoromethylphenyl)-5-(4'-methoxyphenyl)-1,2,4-oxadiazole) able to interfere, upon photo-stimulation, with A β fibrillation, and produce non-toxic oligomers, if treated for appropriate

Acknowledgements

We thank Dr R. Carrota and Dr F. Librizzi for useful discussions; Ing F. D'Anca for technical help in AFM measurements; Dr. A Provenzano and Mr M. Lapis for their technical support; Dr. T. Narayanan and Dr. F. Spinozzi for help in SAXS experiments.

Funding

This work has been supported by Italian grant FIRB "Future in research" RBF12SIPT MIND: "Multidisciplinary Investigations for the development of Neuro-protective Drugs", and Progetto Bandiera N-CHEM.

References

- Cohen, A. S., and Calkins, E. (1959) Electron Microscopic Observations on a fibrous component in Amyloid of diverse origins, *Nature* **183**, 1202–1203.
- Thies, W., and Bleiler, L. (2013) Alzheimer's Association 2013 Alzheimer's disease facts and figures, *Alzheimers Dement.* **9**, 208-245.
- Parihar, M. S., and Hemnani, T. (2004) Alzheimer's disease pathogenesis and therapeutic intervention, *J. Clin. Neurosci.* **11**, 456-467.
- Selkoe, D. J. (2001) Alzheimer's disease: genes, proteins, and therapy, *Physiol Rev* **81**, 741-766.
- Pangalos, M. N., Efthimiopoulos, S., Shioi, J., and Robakis, N. K. (1995) The chondroitin sulphate attachment site of Appican is formed by splicing out exon 15 of the amyloid precursor gene, *J. Biol. Chem.* **270**, 10388-10391.
- Haass, C., and Selkoe, D. J. (1993) Cellular processing of β -amyloid precursor protein and the genesis of amyloid β -peptide, *Cell* **75**, 1039-1042.
- Lorenzo, A., and Yankner, B. A. (1994) Amyloid neurotoxicity requires fibril formation and is inhibited by Congo red, *Proc. Natl. Acad. Sci. USA* **91**, 12243-12247.
- Hoshi, M., Sato, M., Matsumoto, S., Noguchi, A., Yasutake, K., Yoshida, N., and Sato, K. (2002) Spherical aggregates of β -amyloid (amylospheroid) show high neurotoxicity and activate tau protein kinase I/glycogen synthase kinase-3 β , *Proc. Natl. Acad. Sci. USA* **100**, 6370-6375.
- Walsh, D. M., Klyubin, I., J.V., F., Cullen, W. K., Anwyl, R., Wolfe, M. S., Rowan, M. J., and Selkoe, D.-J. (2002) Naturally secreted oligomers of amyloid β -protein potently inhibit hippocampal long-term potentiation in vivo, *Nature* **416**, 483-484.
- Pike, C. J., Burdick, D., and Walencewicz, A. J. (1993) Neurodegeneration induced by beta-Amyloid peptides in vitro: The Role of Peptide Assembly State, *J. Neurosci.* **13**, 1676-1687.
- Kremer, J. J., Pallitto, M. M., Sklansky, D. J., and Murphy, R. M. (2000) Correlation of β -Amyloid Aggregate Size and Hydrophobicity with Decreased Bilayer Fluidity of Model Membranes *Biochemistry* **39**, 10309-10318.
- Lashuel, H. A., Hartley, D., Petre, B. M., Walz, T., and Lansbury, P. T. J. (2002) Amyloid pores from pathogenic mutations, *Nature* **418**, 291-292.
- Walsh, D. M., and Selkoe, D. J. (2004) Oligomers on the brain: the emerging role of soluble protein aggregates in neurodegeneration, *Protein Pept. Lett.* **11**, 213-228.
- Mucke, L., Masliah, E., Yu, G. Q., Mallory, M., Rockenstein, E. M., Tatsuno, G., Hu, K., Kholodenko, D., Johnson-Wood, K., and McConlogue, L. (2000) High-level neuronal expression of $\text{A}\beta$ 1-42 in wild-type human amyloid protein precursor transgenic mice: synaptotoxicity without plaque formation, *J Neurosci.* **20**, 4050–4058.
- Roher, A. E., Chaney, M. O., Kuo, Y. M., Webster, S. D., Stine, W. B., Haverkamp, L. J., Woods, A. S., Cotter, R. J., Tuohy, J. M., Krafft, G. A., Bonnell, B. S., and Emmerling, M. R. (1996) Morphology and toxicity of $\text{A}\beta$ -(1-42) dimer derived from neuritic and vascular amyloid deposits of Alzheimer's disease, *J. Biol. Chem.* **271**, 20631-20635.
- Lambert, M. P., Barlow, A. K., Chromy, B. A., Edwards, C., Freed, R., Liosatos, M., Morgan, T. E., Rozovsky, I., Trommer, B., Viola, K. L., Wals, P., Zhang, C., Finch, C. E., Krafft, G. A., and Klein, W. L. (1998) Diffusible, nonfibrillar ligands derived from $\text{A}\beta$ 1-42 are potent central nervous system neurotoxins, *PNAS* **95**, 6448-6453.
- Hsia, A. Y., Masliah, E., McConlogue, L., Yu, G. Q., Tatsuno, G., Hu, K., Kholodenko, D., Malenka, R. C., Nicoll, R. A., and Mucke, L. (1999) Plaque-independent disruption of natural circuits in Alzheimer's disease mouse models, *Proc. Natl. Acad. Sci. USA* **96**, 3228-3233.
- Necula, M., Kaye, S., Milton, S., and Glabe, C. G. (2007) Small Molecule Inhibitors of Aggregation Indicate That Amyloid β Oligomerization and Fibrillization Pathways Are Independent and Distinct, *J. Biol. Chem.* **282**, 10311-10324.
- Jan, A., Hartley, D. M., and Lashuel, H. A. (2010) Preparation and characterization of toxic $\text{A}\beta$ aggregates for structural and functional studies in Alzheimer's disease research, *Nature Protocols* **5**, 1186-1209.
- Li, M., Yang, X., Ren, J., Qu, K., Qu, X., . (2012) Using Graphene Oxide High Near-Infrared Absorbance for Photothermal Treatment of Alzheimer's Disease, *Adv. Mat.* **24**, 1722-1728.
- Kogan, M. J., Bastus, N.G., Amigo, R., Grillo-Bosch, D., Araya, E., Turiel, A. Labarta, A., Giralt, E., Puentes, V.F. (2006) Nanoparticle-Mediated Local and Remote Manipulation of Protein Aggregation, **6**, 110-115.
- Araya, E., Olmedo, I., Bastus, N.G., Guerrero, S., Puentes, V.F., Giralt, E., Kogan, M.J. (2008) Gold Nanoparticles and Microwave Irradiation Inhibit Beta-Amyloid Amyloidogenesis, *Nanoscale Research Letters* **3**, 435-443.
- Hamley, I. W. (2012) The Amyloid Beta Peptide: A Chemist's Perspective. Role in Alzheimer's and Fibrillation, *Chem. Rev.* **112**, 5147-5192.
- Hawkes, C. A., Ng, V., and McLaurin, J. (2009) Small molecule inhibitors of $\text{A}\beta$ -aggregation and neurotoxicity *Drug Dev. Res.* **70**, 111-124.
- Sgarbossa, A. (2012) Natural Biomolecules and Protein Aggregation: Emerging Strategies against Amyloidogenesis, *Int. J. Mol. Sci.* **13**, 17121-17137.
- Goodman, Y., Steiner, M. R., Steiner, S. M., and Mattson, M. P. (1994) Nordihydroguaiaretic acid protects hippocampal-neurons against amyloid beta-peptide toxicity, and attenuates free-radical and calcium accumulation, *Brain Res.* **654**, 171-176.
- Garcia-Alloza, M., Borrelli, L. A., Rozkalne, A., Hyman, B. T., and Bacskai, B. J. (2007) Curcumin labels amyloid pathology in vivo, disrupts existing plaques, and partially restores distorted neurites in an Alzheimer mouse model, *J. Neurochem.* **102**, 1095–1104.
- Akagawa, M., and Suyama, K. (2001) Amine oxidase-like activity of polyphenols – mechanism and properties, *Eur. J. Biochem.* **268**, 1953-1963.
- Graf, E. (1992) Antioxidant potential of ferulic acid, *Free Radic. Biol Med* **13**, 435-448.
- Kim, H. S., Cho, J. Y., Kim, D. H., Yan, J. J., Lee, H. K., Suh, H. V., and Song, D. K. (2004) Inhibitory effects of long-term administration of ferulic acid on microglial activation induced by intracerebroventricular injection of beta-amyloid peptide (1–42) in mice, *Biol. Pharm. Bull.* **27**, 120-121.
- Butterfields, S., Hejjaoui, M., Fauvet, B., Awad, L., and Lashuel, H. A. (2012) Chemical Strategies for Controlling Protein Folding and Elucidating the Molecular

- Mechanisms of Amyloid Formation and Toxicity, *J. Mol. Biol.* **421**, 204-236.
32. Walsh, D. M., Townsend, M., Podlisny, M. B., Shankar, G. M., Fadeeva, J. V., El Agnaf, O., Hartley, D. M., and Selkoe, D. J. (2005) Certain Inhibitors of Synthetic Amyloid β -Peptide ($A\beta$) Fibrillogenesis Block Oligomerization of Natural $A\beta$ and Thereby Rescue Long-Term Potentiation, *J. Neurosci.* **25**, 2455-2462.
33. Uversky, V. N. (2010) Mysterious oligomerization of the amyloidogenic proteins, *FEBS Journal* **277**, 2940-2953.
34. Ono, K., Hasegawa, K., Naiki, H., and Yamada, M. (2004) Curcumin has potent anti-amyloidogenic effects for Alzheimers beta-amyloid fibrils in vitro, *J. Neurosci. Res* **75**, 742-750.
35. Begum, A. N., Jones, M. R., Lim, G. P., Morihara, T., Kim, P., Heath, D. D., Rock, C. L., Pruitt, M. A., Yang, F., Hudspeth, B., Hu, S., Faull, K. F., Teter, B., Cole, G. M., and Frautschy, S. A. (2008) Curcumin structure-function, bioavailability, and efficacy in models of neuroinflammation and alzheimer's disease, *J. Pharmacol. Exp. Ther.* **326**, 196-208.
36. Anand, P., Kunnumakkara, A. B., Newman, R. A., and Aggarwal, B. B. (2007) Bioavailability of curcumin: problems and promises, *Mol. Pharm.* **4**, 807-818.
37. Yang, C. S., Sang, S., Lambert, J. D., and Lee, M. J. (2008) Bioavailability issues in studying the health effects of plant polyphenolic compounds, *Mol. Nutr. Food. Res.* **52**, 139-151.
38. Narlawar, R., Pickhardt, M., Leuchtenberger, S., Baumann, K., Krause, S., Dyrks, T., Weggen, S., Mandelkow, E., and Schmidt, B. (2008) Curcumin-derived pyrazoles and isoxazoles: Swiss army knives or blunt tools for Alzheimer's disease? , *Chem. Med. Chem.* **3**, 165-172.
39. Orlando, R. A., Gonzales, A. M., R.E., R., L.M., D., and Vander Jagt, D. L. (2012) A Chemical Analog of Curcumin as an Improved Inhibitor of Amyloid Abeta, *Plos One* **7**, e31869. DOI: 31810.31371/journal.pone.0031869.
40. Sgarbossa, A., Monti, S., Lenci, F., Bramanti, E., Bizzarri, R., and Barone, V. (2013) The effects of ferulic acid on β -amyloid fibrillar structures investigated through experimental and computational techniques, *Biochimica et Biophysica Acta* **1830**, 2924-2937.
41. Tarus, B., Straub, J. E., and Thirumalai, D. (2006) Dynamics of Asp23-Lys28 salt-bridge formation in A beta(10-35) monomers, *J. Am. Chem. Soc.* **128**, 16159-16168.
42. Taniguchi, A., Sohma, Y., Kimura, M., Okada, T., Ikeda, K., Hayashi, Y., Kimura, T., Hirota, S., Matsuzaki, K., and Y., K. (2005) "Click Peptide" Based on the "O-Acyl Isopeptide Method": Control of $A\beta$ 1-42 Production from a Photo-Triggered $A\beta$ 1-42 Analogue, *J. Am. Chem. Soc.* **128**, 696-697.
43. Taniguchi, A., Skwarczynski, M., Sohma, Y., Okada, T., Ikeda, K., Prakash, H., Mukai, H., Hayashi, Y., Kimura, T., S., H., Matsuzaki, K., and Y., K. (2008) Controlled Production of Amyloid β Peptide from a Photo-Triggered, Water-Soluble Precursor "Click Peptide", *Chem. Bio. Chem.* **9**, 3055-3065.
44. Bitan, G., and Teplow, D. B. (2004) Rapid Photochemical Cross Linking – A New Tool for Studies of Metastable, Amyloidogenic Protein Assemblies, *Acc. Chem. Res.* **37**, 357-364.
45. Ono, M., Haratake, M., Saji, H., and Nakayama, M. (2008) Development of novel b-amyloid probes based on 3,5-diphenyl-1,2,4-oxadiazole, *Bioorg. Med. Chem.* **16**, 6867-6872.
46. Terenzi, A., Barone, G., Palumbo Piccionello, A., Giorgi, G., Guarcello, A., Portanova, P., Calvaruso, G., Buscemi, S., Vivona, N., and Pace, A. (2010) Synthesis, characterization, cellular uptake and interaction with native DNA of a bis(pyridyl)-1,2,4-oxadiazole copper(II) complex, *Dalton Trans.* **39**, 9140-9145.
47. Palumbo Piccionello, A., Musumeci, R., Cocuzza, C., Fortuna, C. G., Guarcello, A., Pierro, P., and Pace, A. (2012) Synthesis and preliminary antibacterial evaluation of Linezolid-like 1,2,4-oxadiazole derivatives, *Eur. J. Med. Chem.* **50**, 441-448.
48. Fortuna, C. G., Bonaccorso, C., Bulbarelli, A., Caltabiano, G., Rizzi, L., Goracci, L., Musumarra, G., Pace, A., Palumbo Piccionello, A., Guarcello, A., Pierro, P., Cocuzza, C. E. A., and Musumeci, R. (2013) New linezolid-like 1,2,4-oxadiazoles active against Gram-positive multiresistant pathogens, *Eur. J. Med. Chem.* **65**, 533-545.
49. Lentini, L., Melfi, R., Di Leonardo, A., Spinello, A., Barone, G., Pace, A., Palumbo Piccionello, A., and Pibiri, I. (2014) Toward a Rationale for the PTC124 (Ataluren) Promoted Readthrough of Premature Stop Codons: A Computational Approach and GFP-Reporter Cell-Based Assay, *Mol. Pharm.* **11**, 653-664.
50. Vivona, N., Buscemi, S., Pibiri, I., Palumbo Piccionello, A., and Pace, A. (2010) *Synthesis of Heteroaromatics via Rearrangement Reactions*.
51. Buscemi, S., Vivona, N., and Caronna, T. (1995) A generalized and efficient synthesis of 3-amino--5-alkyl-1,2,4-oxadiazoles, 3-(n-alkylamino)-5-alkyl-1,2,4-oxadiazoles, 3-(n,n-dialkylamino)-5-alkyl-1,2,4-oxadiazoles by irradiation of 3-alkanoylamino-4-phenyl-1,2,5-oxadiazoles (furazans), *Synthesis* **8**, 917-919.
52. Buscemi, S., Pace, A., Palumbo Piccionello, A., Pibiri, I., and Vivona, N. (2005) Fluorinated heterocyclic compounds. A photochemical approach to a synthesis of fluorinated quinazolin-4-ones, *Heterocycles* **63**, 1619-1628.
53. Buscemi, S., Pace, A., Palumbo Piccionello, A., Pibiri, I., and Vivona, N. (2005) Fluorinated heterocyclic compounds. A photochemical approach to a synthesis of polyfluoroaryl-1,2,4-triazoles *Heterocycles* **65**, 387-394.
54. Buscemi, S., Pace, A., Vivona, N., Caronna, T., and Galia, A. (1999) Photoinduced single electron transfer on 5-aryl-1,2,4-oxadiazoles: Some mechanistic investigations in the synthesis of quinazolin-4-ones, *J. Org. Chem.* **64**, 728-733.
55. Fezoui, Y., Hartley, D. M., Harper, J. D., Khurana, R., Walsh, D. M., Condron, M. M., Selkoe, D. J., Lansbury, P. T. J., Fink, A. L., and Teplow, D. B. (2000) An improved method of preparing the amyloid beta-protein for fibrillogenesis and neurotoxicity experiments, *Amyloid* **7**, 166-178.
56. Marini, A., Muñoz-Losa, A., Biancardi, A., and Mennucci, B. (2010) What is Solvatochromism? , *J. Phys. Chem. B* **114**, 17128-17135.
57. Kim, J. S., Kodagahally, R., Strekowski, L., and Patonay, G. (2005) A study of intramolecular H-complexes of novel bis(heptamethine cyanine) dyes, *Talanta* **67**, 947-954.
58. Corsale, C., Carrotta, R., Mangione, M. R., Vilasi, S., Provenzano, A., Cavallaro, G., Bulone, D., and San

- Biagio, P. L. (2012) Entrapment of A β 1-40 peptide in unstructured aggregates, *J. Phys. Condens. Matter* *24*, Article Number: 244103.
59. Mylonas, E., and Svergun, D. I. (2007) Accuracy of molecular mass determination of proteins in solution by small-angle X-ray scattering, *J. Appl. Crystallogr.* *40*, 245–249.
60. Ortore, M. G., Spinozzi, F., Vilasi, S., Sirangelo, I., Irace, G., Shukla, A., Narayanan, T., Sinibaldi, R., and Mariani, P. (2011) Time-resolved small-angle x-ray scattering study of the early stage of amyloid formation of an apomyoglobin mutant, *Physical Review E* *84*, doi bita061904.
61. Lu, J. X., Qiang, W., Yau, W. M., Schwieters, C. D., Meredith, S. C., and Tycko, R. (2013) Molecular Structure of β -Amyloid Fibrils in Alzheimer's Disease Brain Tissue, *Cell* *154*, 1257-1268.
62. Pilz, I., Glatter, O., and Kratky, O. (1979) Small-angle X-ray scattering, *Methods Enzymol.* *61*, 148-249.
63. Pedersen, J. S., and Schurtenberger, P. (1996) Scattering Functions of Semiflexible Polymers with and without Excluded Volume Effects, *Macromol.* *29*, 7602-7612.
64. Spinozzi, F., Ferrero, C., Ortore, M. G., De Maria Antolinos, A., and Mariani, P. (2014) GENFIT: software for the analysis of small-angle X-ray and neutron scattering data of macromolecules in solution, *J Appl Crystallogr.* *47*, 1132-1139.

Table of contents

The interaction of oxadiazole **3** photo-stimulated with $A\beta_{1-40}$ induces a structural modification responsible for fibrillogenesis inhibition.

